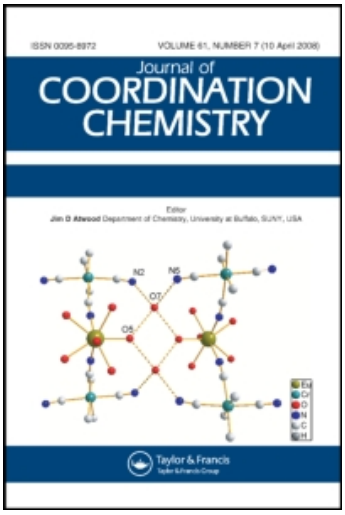

Journal of Coordination Chemistry
Publication details, including instructions for authors and subscription information:
http://www.informaworld.com/smpp/title~content=t713455674

Synthesis, structure, DNA binding and cleavage ability of a new copper ciprofloxacin complex

Yue Wang[a]; Guo-Wu Lin[a]; Jin Hong[a]; Li Li[a]; Yu-Mei Yang[a]; Tao Lu[ab]
[a] College of Basic Science, China Pharmaceutical University, Nanjing 210009, P.R. China [b] Key Laboratory of Drug Quality Control and Pharmacovigilance, China Pharmaceutical University, Ministry of Education, Nanjing 210009, P.R. China

First published on: 14 September 2010

To cite this Article Wang, Yue , Lin, Guo-Wu , Hong, Jin , Li, Li , Yang, Yu-Mei and Lu, Tao(2010) 'Synthesis, structure, DNA binding and cleavage ability of a new copper ciprofloxacin complex', Journal of Coordination Chemistry, 63: 20, 3662 — 3675, First published on: 14 September 2010 (iFirst)
To link to this Article: DOI: 10.1080/00958972.2010.515986
URL: http://dx.doi.org/10.1080/00958972.2010.515986

Journal of Coordination Chemistry
Vol. 63, No. 20, 20 October 2010, 3662–3675

Taylor & Francis
Taylor & Francis Group

Synthesis, structure, DNA binding and cleavage ability of a new copper ciprofloxacin complex

YUE WANG†, GUO-WU LIN†, JIN HONG†, LI LI†,
YU-MEI YANG† and TAO LU*†‡

†College of Basic Science, China Pharmaceutical University, Nanjing 210009, P.R. China
‡Key Laboratory of Drug Quality Control and Pharmacovigilance, China Pharmaceutical University, Ministry of Education, Nanjing 210009, P.R. China

(*Received 22 February 2010; in final form 30 June 2010*)

The structure of **1** consists of $[Cu(HCp)(phen)(H_2O)]^{2+}$ (HCp is ciprofloxacin and phen is 1,10-phenanthroline), two acetates, and four free water molecules. In each cation, copper displays a distorted square pyramid, coordinated to ring 3-carboxylate and 4-oxo oxygen from HCp, two nitrogens from phen, and one water molecule. There are five water molecules in each discrete complex with one coordinated to Cu center, and the other four linked to each other by intermolecular hydrogen bonds. Two uncoordinated acetates make the compound neutral. The complex exhibits higher DNA binding compared to HCp at the same conditions by fluorescence and viscosity measurements. Combining its structure with the DNA-binding result, the binding mechanism may be explained by intercalation. Moreover, **1** shows significant cleavage of DNA in the presence of a reducing agent, such as ascorbate by gel electrophoresis using supercoiled pBR322 DNA in Tris-HCl buffer (pH 7.4). The complex also has a higher activity against Gram-positive bacteria *Staphylococcus aureus* and Gram-negative bacteria *Klebsiella pneumoniae* than HCp.

Keywords: Ciprofloxacin complex; Crystal structure; DNA binding; DNA cleavage

1. Introduction

Quinolones are synthetic antibacterial agents widely used in clinical practice. Ciprofloxacin (1-cyclopropyl-6-fluoro-1,4-dihydro-4-oxo-7-(1-piperazinyl)-3-quinoline carboxylic acid, HCp) is a member of this large family and is regularly found among the top 100 most frequently prescribed drugs in North America, used for the treatment of diseases caused by various Gram-negative and some Gram-positive microorganisms [1].

Exact mechanism of quinolone action is not yet fully understood. It is generally accepted that quinolones represent a large family of synthetic antibacterial agents, which inhibit two important bacterial enzymes, namely DNA gyrases and

*Corresponding author. Email: lut163@163.com

Journal of Coordination Chemistry
ISSN 0095-8972 print/ISSN 1029-0389 online © 2010 Taylor & Francis
DOI: 10.1080/00958972.2010.515986

topoisomerases [2–4]. Several pharmaceutical companies have left the antibiotic discovery field and are much more interested in the more profitable areas of chronic diseases [5, 6]. It is crucial to understand the molecular mode of action of existing drugs, which could help us to exploit them even more efficiently between bacteria and mankind.

Recent studies indicate an important role of metal ions on the mechanism of action of these drugs. The dissociation and coordination behavior of four fluoroquinolone antibiotics (ciprofloxacin, enoxacin, norfloxacin, and ofloxacin) have been studied and published [7–9]. Metal complexes enhance the biological activities of quinolone antibiotics perhaps due to higher liposolubilities leading to greater intracellular accumulations [10–13]. Ciprofloxacin, as the most active representative of this class of quinoline compounds, is studied extensively for the interaction of its complexes with DNA. There are many Cu(II) ciprofloxacin complexes synthesized, such as $[Cu(HCp)(bipy)Cl_{0.7}(NO_3)_{0.3}]NO_3 \cdot 2H_2O$ [14], $[Cu(HCp)_2(ClO_4)_2] \cdot 6H_2O$, $Cu(HCp)_2(NO_3)_2 \cdot 6H_2O$, $Cu(HCp)(C_2O_4) \cdot 2H_2O$ [15], $Cu(HCp)_2(BF_4)_2 \cdot 6H_2O$ [16], $Cu(HCp)_2 \cdot 6H_2O$ [17], $[Cu(HCp)_2Cl_2] \cdot 6H_2O$ [18], $[Cu(HCp)(H_2O)_3]SO_4 \cdot 2H_2O$ [19], $[Cu(HCp)_2(Cu^ICl_2)_2]$, and $[CuCl(HCp)(phen)]Cl \cdot 2H_2O$ [20], where bipy is bipyridine and phen is 1,10-phenanthroline.

In this study, we report the synthesis, crystal structure, DNA binding, and DNA cleavage properties of the Cu(II) complex, $[Cu^{II}(HCp)(phen)(H_2O)]^{2+} \cdot 2CH_3COO^- \cdot 4H_2O$ (**1**). The interaction of **1** with DNA has been investigated using fluorescence and viscosity measurement, and the cleavage was studied by electrophoresis. The complex was tested for potential antibacterial activity.

2. Experimental

2.1. *General remarks*

Analytical grade ciprofloxacin was provided by Sigma, 1,10-phenanthroline and $CuCl_2 \cdot 2H_2O$ were obtained from Shantou Xilong chemical factory. CT DNA was purchased from Sigma. Plasmid pBR322 was purchased from Nanjing Dazhi Biology and Technique Company. Solvents such as methanol were analytical reagents and used as received. Solutions of the metal complex and other reagents for DNA strand scission were prepared fresh daily.

2.2. *Physical measurements*

Elemental analyses were carried out on an Elementar Vario ELIII microanalyzer. Fluorescence spectra were performed with a Shimadzu FR-5301 spectrofluorometer at 25°C. Viscosity experiments were conducted on an Ubbelohde viscometer, immersed in a thermostated water bath at 25°C. Data are presented as $(\eta/\eta_0)^{1/3}$ *versus* the ratio of the concentration of complex and DNA, where η is the viscosity of DNA in the presence of complex and η_0 is the viscosity of DNA alone. Viscosity values were calculated from the observed flow time of DNA-containing solution corrected from the flow time of buffer alone (t_0), $\eta = t - t_0$ [21, 22].

Table 1. Crystal data and structure refinement for **1**.

Chemical formula	$C_{29}H_{28}CuFN_5O_4 \cdot 2CH_3COO \cdot 4H_2O$ ($C_{33}H_{42}CuFN_5O_{12}$)
Formula weight	783.27
Crystal system	Triclinic
Space group	$P2_1/n$ (No. 14)
Unit cell dimensions (Å, °)	
a	10.9095(7)
b	11.5557(7)
c	14.9473(8)
α	71.2271(17)
β	89.7083(19)
γ	76.142(2)
Volume (Å), Z	1726.86(18), 2
Crystal size (mm^3)	$0.4 \times 0.2 \times 0.2$
Shape	Prism
Color	Blue
D_{Calcd} ($g\,cm^{-3}$)	1.506
Reflections collected	7815
Unique reflections	7062
Absorption coefficient (mm^{-1})	0.709
$F(000)$	818.00
$R(F^2 > 2\sigma(F^2))$	0.0348
$wR(F^2)$	0.1001
Goodness-of-fit	1.067
No. of variables	472

2.3. *X-ray structure determination*

X-ray measurements were made on a Rigaku RAXIS RAPID diffractometer with a graphite-monochromated Mo-Kα radiation ($\lambda = 0.71069$ Å) using ω scan mode. A summary of the crystallographic data and structure refinement is given in table 1. The data were corrected for Lorentz and polarization effects. The structure was solved by direct methods [23] using the Crystal Structure [24] software package. The refinement was performed using SHELXTL NT [25]. All hydrogens were located from difference Fourier maps and treated as riding, with C–H distance of 0.93, phenol N–H distance of 0.86, and U_{iso}(H) values equal to 1.2 U_{eq}(C) and U_{iso}(water H) values equal to 1.5 U_{eq}(C) (U_{eq} is the equivalent isotropic displacement parameter for the pivot atom).

The function $\sum w(F_o^2 - F_c^2)^2$ was minimized by using the weighting scheme $w = 1/[\sigma^2(F_o^2) + (aP)^2 + bP]$, where $P = (F_o^2 + 2F_c^2)/3$. Final R [$=\sum(|F_o| - |F_c|)/\sum|F_o|$], Rw[$=(\sum w(|F_o| - |F_c|)^2/\sum w|F_o|^2)^{1/2}$], and S(goodness of fit) [$=(\sum w(|F_o| - |F_c|)^2/(M-N)^{1/2}$), where M = no. of reflections and N = no. of variables used for the refinement] are given in table 1. Anisotropic displacement coefficients were refined for all non-hydrogen atoms. Selected bond distances and angles are listed in table 2.

2.4. *ESI mass spectrometry*

Electrospray interface (ESI) mass spectra were recorded using a Finnigan MAT LCQ iontrap mass spectrometer in the positive ionization mode by loading 1.0 L of solution into the injection valve of the LCQ unit and then injecting into the mobile phase solution (50% of aqueous methanol) which was carried through the ESI into the mass

Table 2. Bond distances (Å) and angles (°) for **1**.

Cu1–O1	1.9238(12)	O1–Cu1–O3	93.75(5)
Cu1–N4	2.0087(14)	O3–Cu1–N4	91.88(5)
Cu1–O4	2.2222(14)	O3–Cu1–N5	168.93(5)
Cu1–O3	1.9487(12)	O1–Cu1–O4	93.99(5)
Cu1–N5	2.0192(14)	N4–Cu1–O4	97.82(5)
		O1–Cu1–N4	166.51(6)
		O1–Cu1–N5	90.42(5)
		N4–Cu1–N5	81.96(6)
		O3–Cu1–O4	94.21(6)

analyzer at a rate of 200 μL min^{-1}. The voltage employed at the electrospray needles was 4.5 kV, N_2 sheath gas flow was 35 units (arbitrary for the LCQ-Deca system), and the capillary was heated to 200°C. A maximum ion injection time of 200 ms along with ten scans was set. The m/z values of metal-anchored species shown in the text represent the most intense peaks in the isotopic distribution. The predicted isotope distribution patterns for complex were calculated using the ISOPRO 3.0 program. All samples were prepared in aqueous solutions containing 20% methanol.

2.5. *Cleavage of pBR322 by the complex*

Reactions were carried out in a total volume of 18 μL by mixing 1 μL of pBR322 plasmid DNA (0.25 μg μL^{-1}), a buffer solution (containing 50 mmol L^{-1} Tris-HCl and 50 mmol L^{-1} NaCl, pH 7.4), and **1** solution in 50% MeOH with ascorbate at a 10-fold molar excess relative to the complex to yield a total volume of 18 μL. The resulting mixtures contain 5×10^{-6} or 5×10^{-5} mol L^{-1} complex. Electrophoresis was carried out at 80 V for 2 h in 0.5XTAE buffer (40 mmol L^{-1} Tris acetate/1 mmol L^{-1} EDTA). The gel was photographed on a capturing system gel printer plus TDI. Bands were quantified using the Scion Image for Windows software program based on NHI Image. By way of comparison, the nuclease activities of HCp, HCp–Cu, and phen–Cu were also tested under the same conditions.

2.6. *Antimicrobial tests*

The minimum inhibitory concentrations (MICs) of ciprofloxacin hydrochloride and its Cu(II) complex against bacterial strains were determined. The MIC was defined as the lowest concentration of antimicrobial agent showing complete inhibition of growth. The MIC of the reference drug (HCp) was compared with its complex. Due to the fact that the MIC values depend on the compound–strain combination, we used the geometric mean MIC values for comparison.

2.7. *Preparation of 1 ($[Cu(HCp)(phen)(H_2O)]^{2+} \cdot 2CH_3COO^- \cdot 4H_2O$)*

HCp (0.1 mmol, 35.5 mg) was dissolved in 6 mL 50% (v/v) methanol–water solution at pH 5 ~ 6 and mixed with methanol solution of phen (0.1 mmol, 20 mg). Then the mixed solution was poured into solid $CuCl_2 \cdot 2H_2O$ (0.1 mmol, 1.7 mg) and reacted for an hour, with its pH adjusted to 5–6 by acetic acid. The solution was placed at room

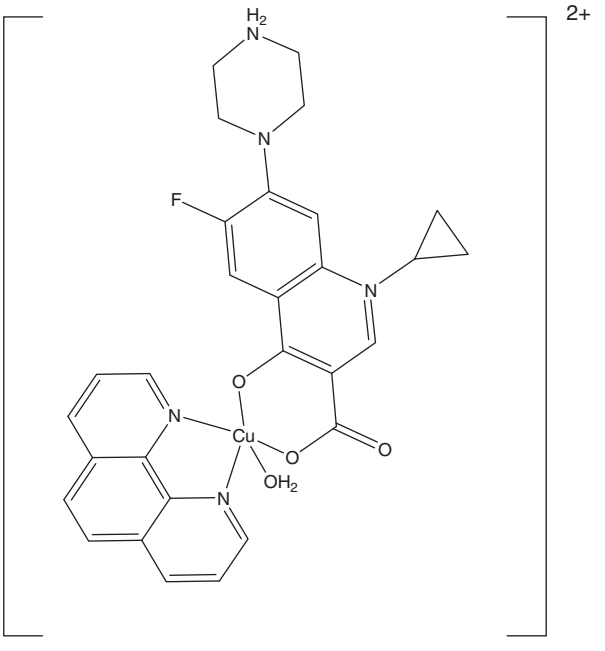

Figure 1. Formula of $[Cu(HCp)(phen)(H_2O)]^{2+}$.

temperature and kept for slow evaporation. Two months later blue prism single crystals of **1** suitable for X-ray diffraction studies were obtained. Elemental Anal. Calcd for $C_{33}H_{42}CuFN_5O_{12}$ (%): C, 50.56; H, 5.36; N, 8.94. Found (%): C, 50.34; H, 5.52; N, 8.69.

3. Results and discussion

3.1. *Structure studies*

The structure of **1** consists of $[Cu(HCp)(phen)(H_2O)]^{2+}$ (figure 1), two acetates, and four free water molecules. In each cation, Cu^{2+} is coordinated to ring 3-carboxylate and 4-oxo oxygens from HCp, phen, and one water molecule in a distorted square pyramid. There are five water molecules in each discrete complex, one coordinated to Cu and the other four are free and linked to each other by intermolecular hydrogen bonds. Two non-coordinated acetates make the compound neutral (figure 2). This structure is very near the analogous complex $[Cu(phen)(nal)(H_2O)]NO_3 \cdot 3H_2O$, where nal is nalidixic acid [26]. The distance between Cu and apical water (Cu–Ow(1) = 2.277(3) Å) is a little longer than the corresponding value (Cu1–O4 = 2.2222(14) Å) in **1** (table 2). Another analogue $[CuCl(C_{17}H_{18}FN_3O_3)(C_{12}H_8N_2)]Cl$ was reported by Drevensek [27] in which HCp is protonated to form a complex ion with the valence of +1. Also, $[Cu(HCp)(phen)Cl]^+$ accompanied by a BF_4 counter anion and four uncoordinated water molecules was reported earlier [28]. After chelating with metal ion, the

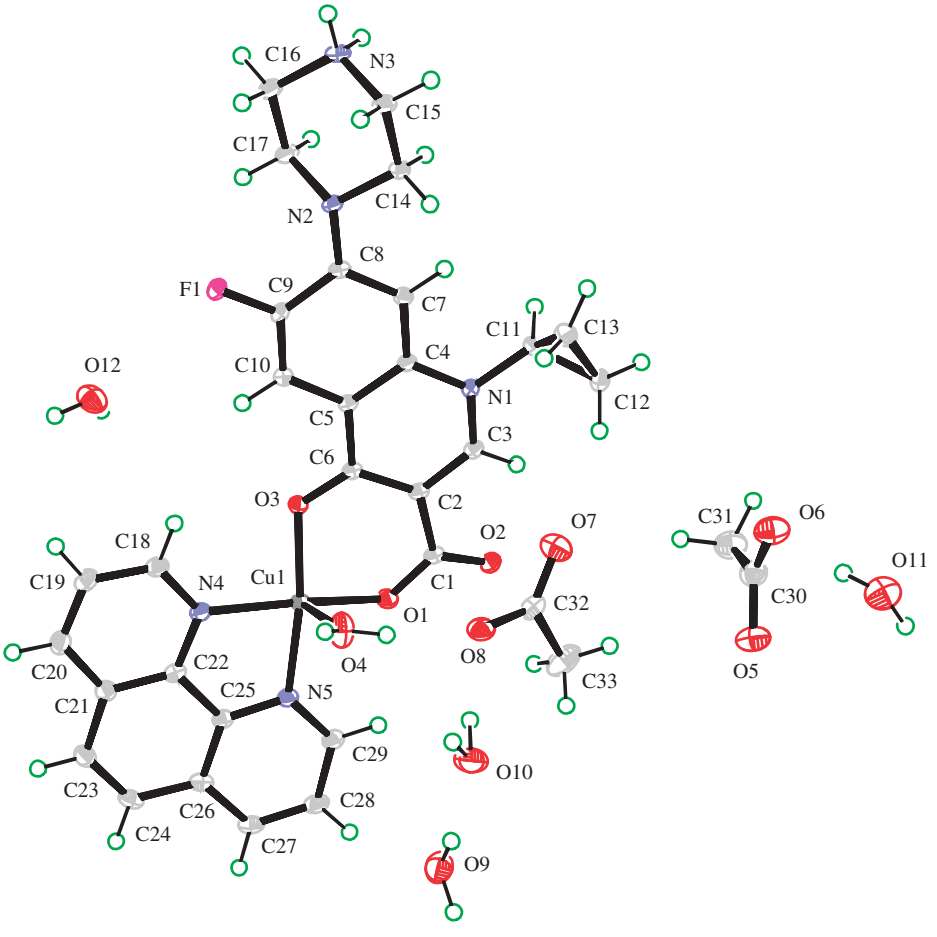

Figure 2. Structure of **1** by XRD, showing 30% probability displacement ellipsoids.

carboxylate of HCp is deprotonated while the imine is protonated to form a thiosine. Compared with the report about the structure of uncoordinated ciprofloxacin salt [29], the length of the C1–O1 and C6–O3 bonds (1.289(2) and 1.275(2) Å, respectively) around the chelating ring in **1** is a little longer than the corresponding bonds (1.2720(17) and 1.2514(6) Å) in free HCp.

The tetragonal geometry with elongated apical bonds is found for Cu(II) in **1**, as expected (Jahn–Teller distorted geometry) for a d_9-Cu(II). The quinolone is more or less planar, with the exception of the cyclopropyl group sticking out of the plane, and the piperazine ring system is in the normal chair conformation. The mean planes of quinolone and phen ligand are nearly coplanar, indicated by the interplanar angle of 6.3°.

Hydrogen bonding also plays an important role in the 3-D structure. The polymeric chains are held together by a network of hydrogen bonds involving coordinated water, crystal lattice water, acetate, and the carboxylate of the ligand.

3.2. *Solution studies*

Figure 3 shows the ESI mass spectrum of **1** which generated two clusters. The major one at m/z 573.17 is assigned to $[Cu + HCp + Phen]^+$, the isotope distribution pattern of which is shown in figure 3(a) and indicate that this ion is singly charged based on the spacing of 1 m/z between the peaks and contains one Cu, which fit very well to the isotope distribution pattern figure 3(c) calculated by ISOPRO 3.0 program. The other at m/z 458.08 is assigned to $[Cu + HCp + 2CH_3OH]^+$, the isotope distribution pattern of which is shown in figure 3(b) and fit figure 3(d) well. So in the solution, the main species is still Cu complex with both ligands.

3.3. *DNA interaction studies*

3.3.1. DNA-binding activity. The binding of the complex to calf thymus (CT) DNA has been studied by fluorescence. Competitive binding studies by measuring the emission of ethidium bromide (EB) bound to DNA show the enhanced emission intensity due to intercalative binding to DNA [30, 31]. Competitive binding of **1** to DNA reduces the emission intensity of EB with either a displacement of the bound EB from the bound to the free state or the bound complex quenching the emission with a reduction of the emission intensity due to fluorescence quenching of free EB [32, 33].

The concentration of DNA, used for binding experiments, was determined by measuring the absorption intensity at 260 nm with the molar extinction coefficient value of 6600 $(mol\,L^{-1})^{-1}\,cm^{-1}$ in 10 mmol L^{-1} Tris-HCl–50 mmol L^{-1} NaCl buffer (pH 7.4) [34]. The interaction of **1** and HCp with DNA was investigated using fluorescence. The fluorescence spectra ($\lambda_{ex} = 545$ nm, $\lambda_{em} = 600$ nm) were recorded at room temperature. In a typical DNA-binding experiment, aliquot of 10 μL 9×10^{-4} mol L^{-1} solution of **1** or HCp were added to the samples containing 2 mL 4.5×10^{-5} mol L^{-1} of DNA and 10 μL 9×10^{-4} mol L^{-1} EB with the complex solution. EB does not show emission in the Tris-buffer medium due to fluorescence quenching by solvent. After the mixtures were incubated for 5 min, their fluorescence-emission intensity had been measured after each addition. The fluorescent emission of EB bound to DNA in the presence of **1** and HCp (figure 4) shows decreasing emission intensity of EB on addition of **1** into the DNA solution. Also, the fluorescence intensities were plotted against **1** and HCp concentration to get a slope that gave the relative extent of binding of two compounds to DNA in figure 5. It is apparent from the plot that EB-bound DNA was efficiently quenched by **1**, in which displacement occurred, indicating that **1** exhibited higher DNA-binding ability than HCp at the same conditions. **1** has a nearly square-planar structure when coordinated water dissociates, which is easy to intercalate to DNA. On the other hand, the positively charged **1** may more easily bind to the negatively charged phosphodiester backbone of DNA. Combining structure with the DNA-binding result, its binding mechanism may be explained mainly by intercalation.

3.3.2. Viscosity measurement. In order to clarify the interactions between complex and DNA, viscosity measurements carried out for optical photophysical probes provide necessary, but not sufficient, clues to support a binding model.

Classical interaction model results in lengthening the DNA helix as base pairs are separated to accommodate the binding ligand, leading to the increase of DNA viscosity.

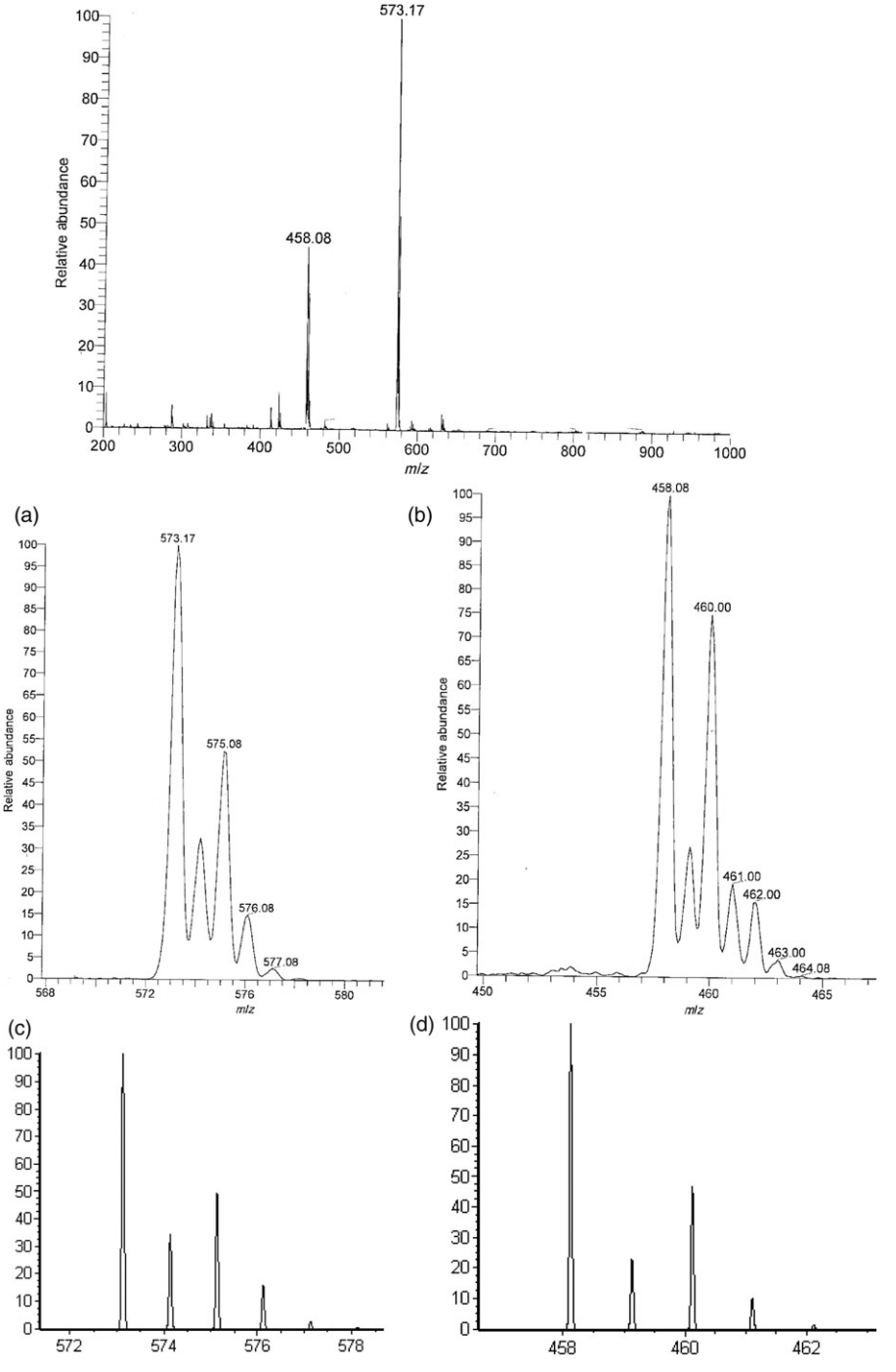

Figure 3. The ESI-MS spectrum of **1**. (a) (*m*/*z* 573.17), (b) (*m*/*z* 458.08) are peaks for coppery species and (c), (d) are isotope distribution pattern for each species, respectively, calculated by ISOPRO 3.0 program.

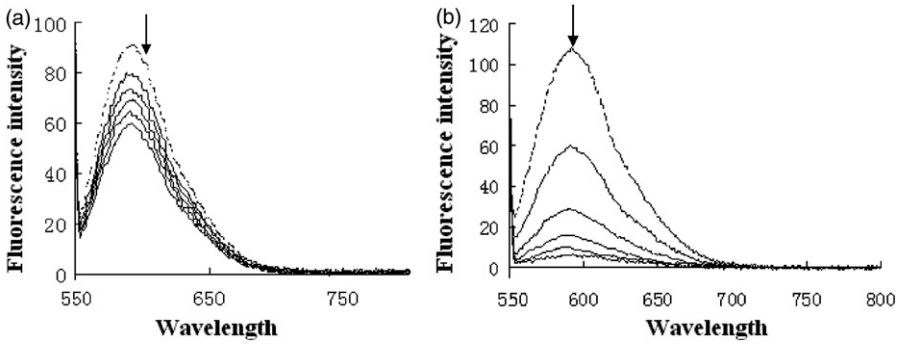

Figure 4. Fluorescence emission spectra (excited at 545 nm) of EB bound to CT DNA in the absence (dashed line) and presence (solid lines) of increasing amounts of 9.0×10^{-4} mol L^{-1} HCp (a) and **1** (b) (10 μL per scan).

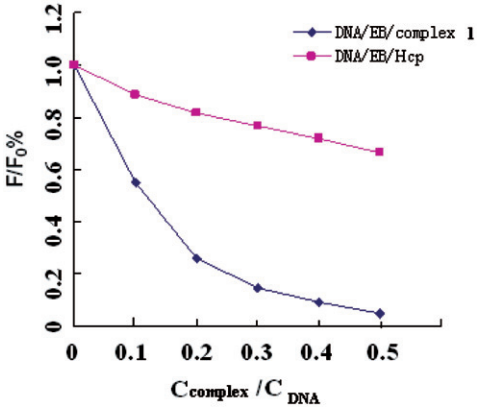

Figure 5. The emission intensity of 4.5×10^{-5} mol L^{-1} CT DNA-bonded EB (4.5×10^{-6} mol L^{-1}) at different concentrations in Tris-HCl buffer (pH 7.4) at 25°C on addition of **1** and HCp.

In contrast, a partial or non-classical interaction of ligand could bend (or kink) the DNA helix, reducing its effective length and, concomitantly, its viscosity [35, 36]. By varying the concentration of added **1** (figure 6), the viscosity of DNA bound to **1** increases, indicating it may intercalate the base pairs of DNA due to increase in the separation of the base pairs at the intercalation sites and, hence, an increase in overall DNA contour length. Thus, we can deduce that **1** shows a very strong DNA-binding ability due to its extended planar structure (coincidence in the solid and solution state) by intercalation.

3.4. *DNA oxidative cleavage*

The metal complex causes random nicks (cuts) to one of the DNA strands. As a consequence, the supercoiled (SC) form opens to form an open circular after one nick

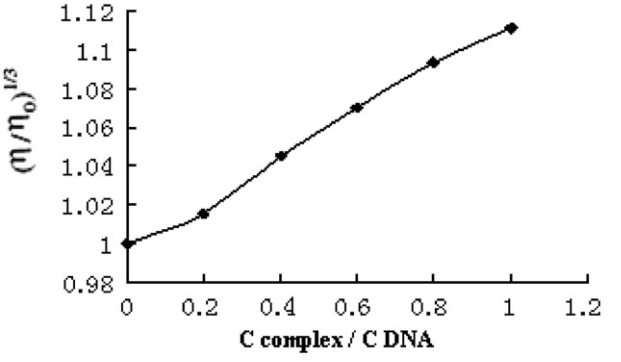

Figure 6. Effect of increasing amounts of **1** on the relative viscosity of DNA.

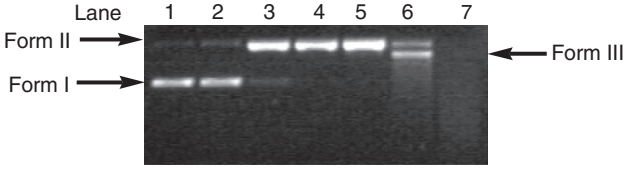

Figure 7. Agarose gel electrophoresis patterns for cleavage of pBR322 plasmid DNA ($0.25\,\mu g\,\mu L^{-1}$) by **1** in the presence of 10-fold excess of ascorbate for 30 min in a buffer solution (containing $50\,mmol\,L^{-1}$ Tris-HCl and $50\,mmol\,L^{-1}$ NaCl, pH 7.4) at 37°C. Key: lane 1, DNA control; lane 2, $c = 1 \times 10^{-6}\,mol\,L^{-1}$; lane 3, $c = 5 \times 10^{-6}\,mol\,L^{-1}$; lane 4, $c = 9 \times 10^{-6}\,mol\,L^{-1}$; lane 5, $c = 1 \times 10^{-5}\,mol\,L^{-1}$; lane 6, $c = 1.5 \times 10^{-5}\,mol\,L^{-1}$; lane 7, $c = 2 \times 10^{-5}\,mol\,L^{-1}$.

and subsequently to a linear form if two nicks on complementary strands are within a short distance. Finally, the DNA gets degraded into small pieces of different sizes which cannot be detected in our assay. The cleavage products were subjected to gel electrophoretic separation and the gels were analyzed after EB staining.

The oxidative DNA cleavage activity of the complex was studied by gel electrophoresis using SC pBR322 DNA in Tris-HCl buffer (pH 7.4) in the presence of a reducing agent, ascorbate. Complex **1** shows significant cleavage of DNA in the presence of ascorbate. Control experiment done under the same conditions does not show any apparent cleavage activity. With the increasing concentration of **1**, the DNA-cleavage propensity is enhanced (figure 7); the oxidative cleavage data are listed in table 3. The best cleavage result was obtained at $1.5 \times 10^{-5}\,mol\,L^{-1}$, when degradation to the linear form was observed. With higher concentration, the linear form almost disappeared to footprint for it is furthermore degraded to small pieces in lane 7. The nuclease activity of **1** at $1 \times 10^{-5}\,mol\,L^{-1}$ is comparable to that of phen, phen–Cu(II), and HCp–Cu(II) obtained according to the reported method [15, 37]. [$Cu(phen)_2^{2+}$] has high nucleophilic efficiency for Cu(II) complex reduced to Cu(I) complex and then bound to the small groove of DNA by attacking C-1′ H or C-4′ H, while in this case its cleavage efficiency is lower than **1**. From figure 8 and data listed in table 4, we deduce that all compounds have some nuclease activity but at the same concentration, **1** shows the highest cleavage efficiency (lane 6 in figure 8) which coincides with its high DNA-binding property with the large planar structure.

Table 3. Oxidative cleavage data of SC pBR322 by **1**.

Lane	Concentration (mol L^{-1})	SC (%)	Nicked (%)	Linear (%)
1	DNA control	91.75	8.25	
2	1×10^{-6}	85.23	14.77	
3	5×10^{-6}	11.54	88.46	
4	9×10^{-6}	2.37	97.63	
5	1×10^{-5}		100	
6	1.5×10^{-5}		72.39	27.61
7	2×10^{-5}			

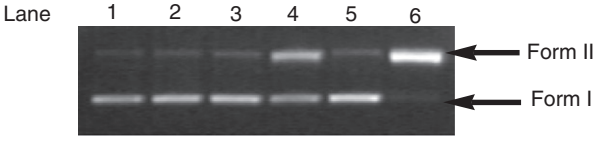

Figure 8. Agarose gel electrophoresis patterns for the cleavage of pBR322 plasmid DNA (0.25 μg μL^{-1}) by phen–Cu(II), HCp–Cu(II), or **1** and ligand (phen or HCp) in the presence of 10-fold excess of ascorbate for 30 min in a buffer solution (containing 50 mmol L^{-1} Tris-HCl and 50 mmol L^{-1} NaCl, pH 7.4) at 37°C. Key: lane 1, DNA control; lane 2, phen (1×10^{-5} mol L^{-1}); lane 3, HCp (1×10^{-5} mol L^{-1}); lane 4, Phen–Cu(II) (1×10^{-5} mol L^{-1}); lane 5, HCp–Cu(II) (1×10^{-5} mol L^{-1}); lane 6, **1** (1×10^{-5} mol L^{-1}).

Table 4. Comparison of oxidative cleavage data of SC pBR322 by complexes at 1×10^{-5} mol L^{-1}.

Lane	Compounds	SC (%)	Nicked (%)	Linear
1	DNA control	91.85	8.15	
2	Phen	86.59	13.41	
3	HCp	84.96	15.04	
4	Phen–Cu(II)	36.72	63.28	
5	HCp–Cu(II)	86.35	13.65	
6	**1**	1.81	98.19	

Table 5. MIC (μg mL^{-1}) of the drugs for standard assayed bacteria.

	MIC (μg mL^{-1})	
Microorganism	**1**	HCp
S. aureus ATCC25923	6.25	3.65
E. coli ATCC25922	1.25	3.65
P. aeruginosa ATCC27853	1.25	9.125
S. paratyphi ACMCC(B) 50071	6.25	9.125
Bacillus dysenteriae CMCC(B) 51302	<0.079	0.0365

3.5. *Antimicrobial tests*

Tables 5 and 6 show the MICs of ciprofloxacin and **1** against standard strains and clinic Gram-positive and Gram-negative bacteria, respectively. By comparison, **1** shows high bactericidal activity against the standard strains of *Escherichia coli* ATCC25922,

Table 6. MIC ($\mu g\,mL^{-1}$) of the drugs for Gram-positive and negative–positive assayed bacteria.

Microorganism		Drug	MIC ($\mu g\,mL^{-1}$) MIC_{50}	MIC ($\mu g\,mL^{-1}$) MIC_{90}
Gram-positive bacteria	*S. aureus*	**1**	18.25	>64
		HCp	25	>64
	S. epidermidis	**1**	9.125	>64
		HCp	6.25	>64
Gram-negative bacteria	*Bacillus dysenteriae*	**1**	9.125	9.125
		HCp	6.25	9.125
	Bacterium coli	**1**	>64	>64
		HCp	>64	>64
	K. pneumoniae	**1**	3.65	9.125
		HCp	6.25	6.25

Pseudomonas aeruginosa ATCC27853, and *Salmonella paratyphi* ACMCC(B) 50071. **1** has higher activity against Gram-positive bacteria *Staphylococcus aureus* and Gram-negative bacteria *Klebsiella pneumoniae* than the HCp itself.

4. Conclusion

One copper ciprofloxacin complex, **1**, with two acetates was synthesized and its crystal structure determined. Its activity with DNA was measured systematically by fluorescence, viscosity, and gel electrophoresis. Complex **1** exhibited higher DNA-binding ability compared to the HCp at the same condition. Combining its structure with the DNA-binding result, the binding mechanism may be explained mainly by intercalation. Also, **1** showed significant cleavage of DNA in the presence of the reducing agent ascorbate by gel electrophoresis using SC pBR322 DNA in Tris-HCl buffer (pH 7.4). Moreover, **1** had higher activity against *S. aureus* and *K. pneumoniae* than HCp itself. Although many related metal fluoroquinolone complexes have been published [38–40], our systematic study including the research from the solid structure to the formation in the solution state, from DNA-binding to DNA-cleavage ability, and antimicrobial tests of HCp copper complex, is seldom reported. The comprehensive results would provide more information for the development of metal complexes of quinolones.

Supplementary material

The final atomic coordinates, anisotropic displacement coefficients, bond lengths, bond angles, torsion angles of non-H atoms, and the atomic coordinates of H atoms have

been deposited in the Cambridge Crystallographic Data Centre, Cambridge University Chemical Laboratory, Cambridge CB21EW, U.K. (CCDC 666425 for **1**).

Acknowledgments

We thank Prof. Okabe N. and Dr Odoko M. of Kinki University in Japan for X-ray technical assistance. The Project is sponsored by the Scientific Research Foundation for the Returned Overseas Chinese Scholars, State Education Ministry.

References

[1] J.E.F. Reynolds. *Martindale, The Extra Pharmacopeia*, 30th Edn, p. 145, Pharmaceutical Press, London (1993).
[2] L.A. Mitscher. *Chem. Rev.*, **105**, 559 (2005).
[3] T.D. Gootz, J.F. Barrett, J.A. Sutcliffe. *Antimicrob. Agents Chemother.*, **34**, 8 (1990).
[4] K. Hoshino, A. Kitamura, I. Morrissey, K. Sato, J. Kato, H. Ikeda. *Antimicrob. Agents Chemother.*, **38**, 2623 (1994).
[5] Available online at: http://www.nature.com/news/2004/041018/pf/431892a_pf.html, doi:10.1038/431892a
[6] S.B. Levy. *Adv. Drug Delivery Rev.*, **57**, 1446 (2005).
[7] D.S. Lee, H.J. Han, K. Him, W.B. Park, J.K. Cho, J.H. Kim. *J. Pharm. Biomed. Anal.*, **12**, 157 (1994).
[8] E.K. Efthidou, A. Karaliota, G. Psomas. *J. Inorg. Biochem.*, **104**, 455 (2010).
[9] L.C. Yu, L. Lai, R. Xia, S.L. Liu. *J. Coord. Chem.*, **62**, 1313 (2009).
[10] J.R. Anacona, C. Toledo. *Transition Met. Chem.*, **26**, 228 (2001).
[11] N. Ramirez-Ramirez, G. Mendoza-diaz, F. Gutiérrez-Corona, M. Pedraza-Reyes. *Bioinorg. Chem.*, **3**, 188 (1998).
[12] E.B. Jakics, S. Iyobe, K. Hirai, H. Fukuda, H. Hashimoto. *Antimicrob. Agents Chemother.*, **36**, 2562 (1992).
[13] K. Timmers, R. Sternglanz. *Bioinorg. Chem.*, **9**, 145 (1978).
[14] S.C. Wallis, L.R. Gahan, B.G. Charles, T.W. Hambley, P.A. Duckworth. *Inorg. Biochem.*, **62**, 1 (1996).
[15] N. Jiménez-Garridoa, L. Perelló, R. Ortiz, G. Alzuet, M. González-Álvarez, E. Cantón, M. Liu-González, S. García-Granda, M. Pérez-Priede. *Inorg. Biochem.*, **99**, 677 (2005).
[16] D.K. Saha, S. Padhye, C.E. Anson, A.K. Powell. *Inorg. Chem. Commun.*, **5**, 1022 (2002).
[17] M.P. López-Gresa, R. Ortiz, L. Perelló, J. Latorre, M. Liu-González, S. García-Granda, M. Pérez-Priede, E. Cantón. *Inorg. Biochem.*, **92**, 65 (2002).
[18] I. Turel, I. Leban, N. Bukovec. *Inorg. Biochem.*, **56**, 273 (1994).
[19] I. Turel, L. Golič, O.L. Ruiz Ramirez. *Acta Chim. Slov.*, **46**, 203 (1999).
[20] P. Drevenšek, T. Zupančič, B. Pihlar, R. Jerala, U. Kolitsch, A. Plaper, I. Turel. *Inorg. Biochem.*, **99**, 432 (2005).
[21] M. Eriksson, M. Leijon, C. Hiort, B. Norden, A. Graeslund. *Biochemistry*, **3**, 5031 (1994).
[22] Y. Xiong, X.F. He, X.H. Zou, J.Z. Wu, X.M. Chen, L.N. Ji, R.H. Li, J.Y. Zhou, K.B. Yu. *J. Chem. Soc., Dalton Trans.*, 19 (1999).
[23] A. Altomare, M.C. Burla, M. Camalli, G.L. Cascarano, C. Giacovazzo, A. Guagliardi, A. Moliterni, G. Polidori, R. Spagna. *J. Appl. Cryst.*, **32**, 115 (1999).
[24] *Crystal Structure Analysis Package*, Rigaku and Rigaku/MSC(2000–2004). 9009 New Trails Dr., The Woodlands, TX 77381, USA.
[25] G.M. Sheldrick. *SHELXTL NT Version 5.1, Program for Solution and Refinement of Crystal Structures*, University of Göttingen, Germany (1997).
[26] G. Mendoza-Díaz, L.M.R. Martinez-Aguilera, R. Perez-Alonso. *Inorg. Chim. Acta*, **138**, 41 (1987).
[27] P. Drevensek, I. Leban, I. Turel, G. Giester, E. Tillmanns. *Acta Cryst.*, **C59**, m376 (2003).

[28] D.K. Saha, S. Patitungkho, S. Padhye, D.N. Deobagkar, A. Ozarkar, M.M. Bhadbhade, R.G. Gonnade. *Transition Met. Chem.*, **30**, 334 (2005).
[29] X. Li, Y. Hu, Y. Gao, G.G.Z. Zhang, R.F. Henry. *Acta Cryst.*, **E62**, o5803 (2006).
[30] J.B. Le Pecq, C. Paoletti. *J. Mol. Biol.*, **27**, 87 (1967).
[31] M.J. Waring. *J. Mol. Biol.*, **13**, 269 (1965).
[32] A.M. Thomas, A.D. Naik, M. Nethaji, A.R. Chakravarty. *Inorg. Chim. Acta*, **357**, 2315 (2004).
[33] S. Mahadevan, M. Palaniandavar. *Inorg. Chem.*, **37**, 3927 (1998).
[34] M.E. Reichman, S.A. Rice, C.A. Thomas, P. Doty. *J. Am. Chem. Soc.*, **76**, 3047 (1954).
[35] X.H. Zou, B.H. Ye, H. Li, J.G. Liu, Y. Xiong, L.N. Ji. *J. Chem. Soc., Dalton Trans.*, 1423 (1999).
[36] D.S. Sigma, A. Mazumder, D.M. Perrin. *Chem. Rev.*, **93**, 2295 (1993).
[37] B.Q. Ma, S. Gao, T. Yi, C.H. Yan, G.X. Xu. *Inorg. Chem. Commun.*, **3**, 93 (2000).
[38] L.C. Yu, Z.L. Tang, P.G. Yi, S.L. Liu, X. Li. *J. Coord. Chem.*, **62**, 903 (2009).
[39] L.C. Yu, L. Lai, S.L. Lin, Y. Xia. *J. Coord. Chem.*, **62**, 2261 (2009).
[40] L.C. Yu, Z.L. Tang, P.G. Yi, S.L. Liu. *J. Coord. Chem.*, **62**, 894 (2009).